

# A half subcarrier guard band spectrum assignment scheme for multi-user FBMC systems

Wei Huang<sup>1,2</sup>, Hongbo Xu<sup>3</sup>, and Zhongnian Li<sup>3\*</sup>

<sup>1</sup> College of Information and Communication Engineering, Harbin Engineering University, Harbin, 100051 China

<sup>2</sup> Low Frequency Electromagnetic Communication Laboratory, Wuhan Marine Communication Research Institute, Wuhan, 430205 China  
[e-mail: wolf185269571@163.com]

<sup>3</sup> Department of Electronics and Information Engineering, Central China Normal University, Wuhan, 430079 China  
[e-mail: zhongnian.li@mail.ccnu.edu.cn]

\*Corresponding author: Zhongnian Li

*Received November 15, 2021; accepted December 25, 2021;  
published January 31, 2022*

---

## Abstract

Traditionally, in multi-user multi-carrier systems, the neighboring subband will be gapped by one subcarrier, which is set as guard band to reduce multiple access interference (MAI) between neighboring subbands. The empty subcarrier for guard band will degrade the spectral efficiency of the whole system. In order to enhance the spectral efficiency of multi-user filter bank multiple carrier (FBMC) systems, a new subband allocation method is introduced, in which the neighboring subband is gapped by half subcarrier instead of one subcarrier. Meanwhile, in order to implement the proposed resource allocation scheme, an optimized FBMC prototype filter is designed to decrease the inter-subband interference to the neighboring subband. The detailed simulations about the comparison between the proposed spectrum assignment and traditional FBMC are given, as well as the performance in the different interference scenarios. The simulation results show that the combination of the proposed spectrum assignment scheme and the optimized filter has better performance compared to the traditional scheme. The proposed scheme can be used in the system which serves massive users to get higher spectrum efficiency.

---

**Keywords:** filter bank multiple carrier, frequency guard band, half subcarrier gap, multiple access interference, optimized prototype filter

## 1. Introduction

**F**ilter bank multiple carrier (FBMC) is a potential transmission waveform compared to the traditional orthogonal frequency division multiplexing (OFDM) used in the fourth and fifth generation mobile system [1-3]. The flexible prototype filter used in FBMC has more advantages compared to the rectangle filter used in OFDM to resist the doubly selective channel [4]. Furthermore, due to no need of CP (cyclic prefix) used in OFDM, FBMC has higher spectrum efficiency than OFDM.

Generally, there are three different types of prototype filter: filtered multi-tone (FMT), cosine-modulated multi-tone (CMT) and staggered modulated multi-tone (SMT) [5]. The FMT transmission has lower spectral efficiency since the spectrum is not overlapped. Meanwhile, CMT and SMT have the same higher spectral efficiency, and can transform into each other in some aspects [6]. Therefore, SMT and CMT have been widely used. SMT is also called orthogonal frequency division multiplexing offset quadrature amplitude modulation (OFDM/OQAM) due to its overlapped spectrum. If OFDM/OQAM is used as the basic transmission waveform, the multiple access based on OFDM/OQAM should be considered [7] [8].

In the traditional multiple access systems (multi-user scenario), since the spectrum of signal is not deeply sharp, the guard band in frequency domain is needed to mitigate the multiple access interference (MAI) in frequency division multiple access (FDMA), also in OFDMA systems based on OFDM waveform [9]. The greater number of guard band is in use, the better performance against MAI to get, but the lower number of subcarriers is available for data transmission in the OFDMA systems.

If massive users have been served in one system (e.g. Massive Machine Type Communication (mMTC) in 5G), many subcarriers will be used for guard band, which will greatly degrade the spectrum efficiency of the whole system.

Meanwhile, in OFDM/OQAM multiple access system, considering that it is still a multiple carrier system, the guard band can be also set as one subcarrier as usually in OFDM system [10-12]. The scheme of one subcarrier for guard band can works, but OFDM/OQAM has its specialty due to its flexible prototype filter. There are some works to enhance the spectral efficiency. In [13], it does not need guard band to improve the spectral efficiency, but it changes the structure of OFDM/OQAM using a single band filter on the edge subcarrier.

Considering the prototype filter in OFDM/OQAM can be optimized according to the requirements, for example, the bandwidth of the main lobe and the amplitude of side lobe can be adjusted [14], we propose a scheme that the guard band is set as half subcarrier gap to enhance the spectrum efficiency without changing the structure. To match this scheme, an optimized prototype filter is also put forwarded.

In FBMC systems, there are many famous prototype filters, such as a square root raised-cosine filter (SRRC), IOTA, Hermit filter [15], PHYDYAS [16]. Every prototype filter has different characteristics to adapt the channel parameters, i.e., multiple path delay spread, doppler frequency shift. This paper also sparkles this idea on the multiple user system, resource allocation. The new prototype filter can be designed to adapt the new application scenario.

The rest of the paper is organized as follows. In section 2, the traditional transmission methods adopted in the multi-user scenario are described and the new half subcarrier gap scheme is put forward. In section 3, the optimized filter used in the scenario is presented. In section 4, the simulations are conducted and analyzed. Finally, the conclusions are drawn in section 5.

## 2. System Model

### 2.1 FBMC Model

FBMC system is a multi-carrier system. It's transmitted symbol  $s[m]$  is denoted as

$$s[m] = \sum_{k=0}^{M-1} \sum_{n \in \mathbb{Z}} d_{k,n} g_{k,n}[m], \quad (1)$$

in which,  $M$  is the number of subcarriers,  $d_{k,n}$  is the transmitted data on  $k$ -th subcarrier and  $n$ -th time interval.  $g_{k,n}[m]$  is the shifted version of the prototype filter  $g[m]$  in time and frequency domain, which is depicted as

$$g_{k,n}[m] = (-1)^{kn} e^{-j\frac{\pi k}{M}(L_p-1)m} e^{j\frac{2\pi}{M}km} g[m - n\frac{M}{2}]. \quad (2)$$

$L_p$  is the length of the prototype filter  $g[m]$ .

At the receiver, FBMC system uses the same filter to recover the data.

$$\begin{aligned} d'_{k,n} &= \langle s[m], g_{k,n}[m] \rangle = \sum_{m=-\infty}^{\infty} s[m] g_{k,n}^*[m] \\ &= \sum_{k'=0}^{M-1} \sum_{n' \in \mathbb{Z}} d_{k',n'} \left( \sum_{m=-\infty}^{\infty} g_{k',n'}[m] g_{k,n}^*[m] \right) \end{aligned} \quad (3)$$

If ambiguity function  $A_p(k, n)$  [4] of prototype filter  $g[m]$  satisfies

$$A_p(k, n); \sum_{m=-\infty}^{\infty} g_{k',n'}[m] g_{k,n}^*[m] = \begin{cases} 1, & k=0, n=0 \\ 0, & \text{else} \end{cases}, \quad (4)$$

the original data will be recovered. i.e.,  $d'_{k,n} = d_{k,n}$ .

Unfortunately, for FBMC, the equation is not satisfied due to the prototype filter  $g[m]$ . However, the delicate designed prototype filter  $g[m]$  in FBMC, such as PHYDYAS, IOTA filter, only the real part (Re operation) of their ambiguity function  $A_p(k, n)$  satisfies

$$\text{Re} \left[ \sum_{m=-\infty}^{\infty} g_{k',n'}[m] g_{k,n}^*[m] \right] = \begin{cases} 1, & k=0, n=0 \\ 0, & \text{else} \end{cases}. \quad (5)$$

In this way,  $d_{k,n}$  should be pure real value. However, complex value is our transmission data. So, complex value should be decomposed as two real value. i.e.,  $c_{k,n} = d_{k,n} + jd_{k,n+1}$ . In order to save transmission time, the real part of symbol and the imaginary part should be transmitted in staggered ways. Therefore, we call this type FBMC as SMT.

From the discussion above, the prototype filter is the key of FBMC systems. Compared to the rectangle pulse in OFDM, the prototype filter in current FBMC has better characteristic of joint time-frequency localization, it has better performance on doubly selective channel than OFDM. Now, many prototype filters have been designed used in different scenario [17]. Furthermore, paper [14] proposed a method to design new prototype filter to accommodate the different scenario. However, to the knowledge of author, the prototype filter for multi-user consideration is not mentioned before.

### 2.2 Multi-user model

In multi-user systems, there will be multiple access interference between different users in different resource group, as well as intra-band interference if multi-stream is considered.

For simplicity, a downlink multi-user MIMO-FBMC system is shown in Fig. 1, in which, a base station with two transmit antennas serves six users with only one antenna each. Furthermore, six users are divided into three groups, i.e., user 1 and user 2 are in group 1, which receives data on the subband 1 composed by several subcarriers. Similarly, user 3 and user 4 comprise group 2, which uses the subband 2. User 5 and user 6 are in group 3, which uses the subband 3.

Obviously, in every group, there will be intra-band interference since two users use the same resource. Meanwhile, there will also have inter-band interference if the guard band is not considered.

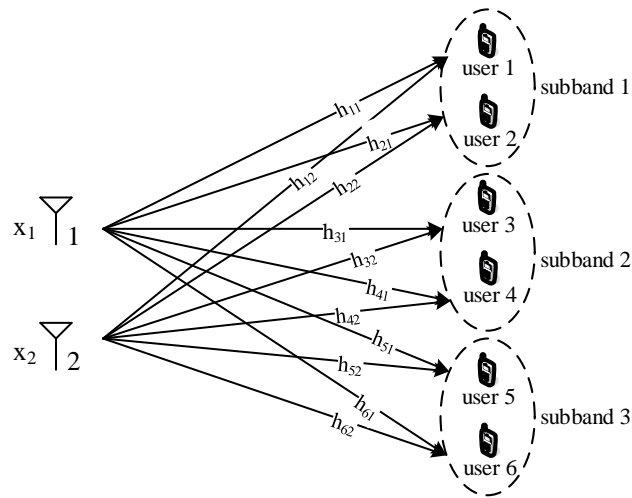


Fig. 1. System model for multi-user system

The channel response matrix  $H_1$  in subband 1,  $H_2$  in subband 2 and  $H_3$  in subband 3 are shown as follows,

$$\begin{aligned} H_1 &= \begin{bmatrix} h_{11} & h_{12} \\ h_{21} & h_{22} \end{bmatrix}, \\ H_2 &= \begin{bmatrix} h_{31} & h_{32} \\ h_{41} & h_{42} \end{bmatrix}, \\ H_3 &= \begin{bmatrix} h_{51} & h_{52} \\ h_{61} & h_{62} \end{bmatrix}, \end{aligned} \quad (6)$$

in which, the matrix element  $h_{ij}$  is the channel response from transmit antenna  $j$  to user  $i$ . Since the locations of users are different, the channel response matrices are independent.

In each group, the two users use the same frequency band and will interfere each other. Therefore, for simplicity, zero-forcing (ZF) precoding algorithm is adopted to separate two users in each subband easily, which lead to no intra-band interference. Then, the transmitted signals in each subband are as follows,

$$\begin{aligned} X_1 &= \begin{bmatrix} x_1 \\ x_2 \end{bmatrix} = (H_1)^+ \begin{bmatrix} s_1 \\ s_2 \end{bmatrix}, \\ X_2 &= \begin{bmatrix} x_3 \\ x_4 \end{bmatrix} = (H_2)^+ \begin{bmatrix} s_3 \\ s_4 \end{bmatrix}, \\ X_3 &= \begin{bmatrix} x_5 \\ x_6 \end{bmatrix} = (H_3)^+ \begin{bmatrix} s_5 \\ s_6 \end{bmatrix}, \end{aligned} \quad (7)$$

in which,  $s_i (i=1,2,3,4,5,6)$  is the data of user  $i$  and  $(H_i)^+$  is the pseudo inverse matrix of  $H_i$ , i.e.,  $(H_i)^+ H_i = I$ . Then, the transmitted signal  $X$  will be modulated in FBMC waveform.

In this scenario, the user 3 in group 2 is our focus, because it has more interference than other users. User 3 will experience intra-band interference from user 4, but this interference can easily be cancelled by ZF algorithm. Not only intra-band interference, User 3 will also experience the severe interference from other group user 1, 2, 5, 6, which is called as the inter-band interference (i.e., MAI), if their signal spectrums are overlapped.

The different transmission methods of multiple access are shown in Fig. 2. If the FMT transmission in Fig. 2 (a) is adopted, it is obvious that there is very small inter-band interference since the main lobe of spectrum is not overlapped. But it has lower spectral efficiency compared to traditional FBMC (SMT) since the main lobes of SMT are overlapped.

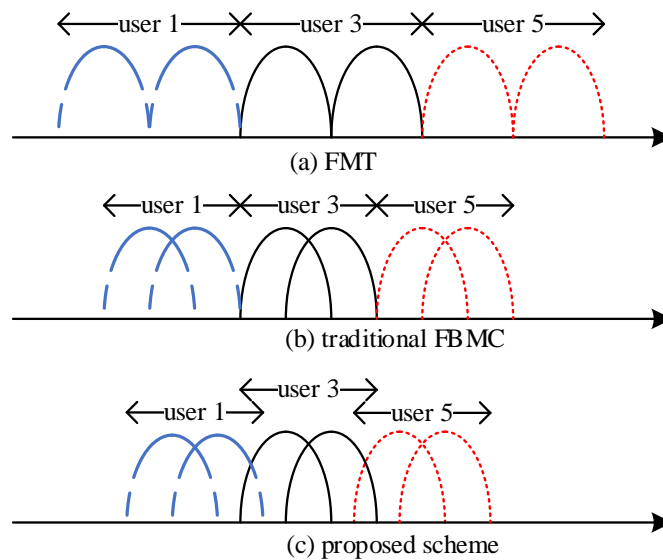


**Fig. 2.** The comparison of the different transmission methods (it is assumed that a subband will cover two subcarriers and only main lobe is shown.)

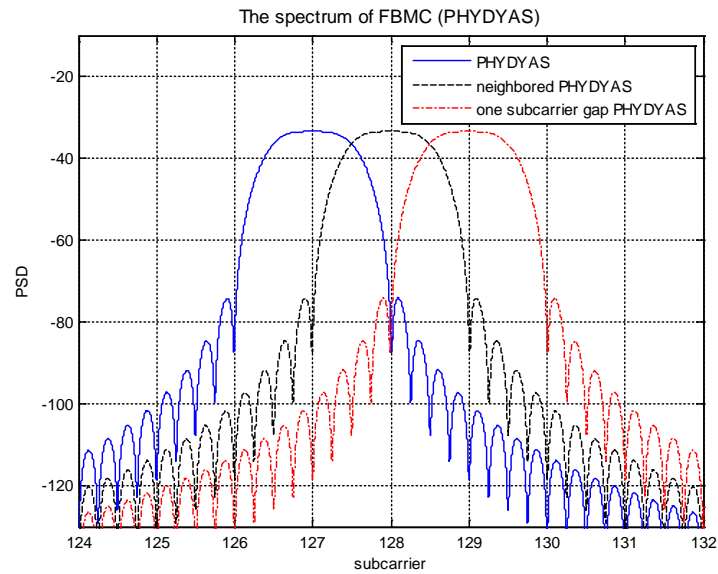


**Fig. 3.** The spectrum of FBMC (PHYDYAS)

As for SMT, set the widely used PHYDYAS prototype filter as the example, the spectrum of one subband almost covers two subcarriers, which is shown in **Fig. 3**.

If the guard band between the neighboring subband is zero (i.e., the solid blue line curve and the dashed black line curve), the neighboring subband spectrums will greatly overlap. Due to uncertainty of the neighboring subband channel response on different users, the overlapped interference cannot be cancelled resulting that the interference from neighboring subband of different user is very large to worsen the performance.

If the guard gap between the neighboring subbands is larger than one subcarrier (i.e., the solid line blue curve and the dash-dot red line curve), the MAI interference will be very small because it only has side lobe interference instead of main lobe interference. Since the power of the side lobe will lower than main lobe at almost 40dB [4], the MAI interference from side lobes will be neglected.

Therefore, in traditional multi-user spectrum resource assignment, the neighboring subband is gapped by usually one subcarrier in FBMC [8, 10], which is shown in **Fig. 2 (b)**. In one subband, two subcarriers are overlapped. Between two subbands, no overlap exists. This kind of scheme is usually used in OFDM systems. However, the gaped empty subcarrier is not used for data transmission, which will degrade the system spectrum efficiency.

Considering trying to enhance the spectrum efficiency, we put forward half subcarrier gaped subband assignment scheme, i.e., the neighboring subband is gaped by half subcarrier as shown in **Fig. 2 (c)**. This scheme also means the neighboring subbands are overlapped by half subcarrier, which will bring MAI interference, but we can make the MAI interference at a lower level not to greatly degrade the quality of communication. Meanwhile, to match the half subcarrier scheme to alleviate the MAI interference at a lower level, a prototype filter is optimized.

### 3. The optimized prototype filter

From the Fig. 2 (c), the neighboring subband spectrums gapped by half subcarrier still overlap resulting that it still has inter-subband interference to each other subband. However, we can design a delicate prototype filter to make this interference not to degrade the performance sharply. Therefore, in order to have smaller guard band, the energy of the overlapped band should be decreased. According to the paper [14], with the non-perfect reconstruction (NPR) constraint, the corresponding optimized rule is as follows,

$$\begin{aligned} \min_{h(0), h(1), \dots, h(L_p-1)} & \int_{w_0}^{\pi} |H(e^{jw})|^2 dw, \\ \text{s.t.} & \begin{cases} h(l) = h(L_p - 1 - l), l = 0, 1, \dots, L_p - 1, \\ \text{Power}(I_{k,n}^a) < TH, \\ \text{Power}(I_{k,n}^b) < TH, \\ \sum_{l=0}^{L_p-1} (h(l))^2 = 1, \end{cases} \end{aligned} \quad (8)$$

where  $I_{k,n}^a$  and  $I_{k,n}^b$  are ISI/ICI interference to the real part and imaginary part of the data  $d_{k,n}$ , respectively.  $N$  is the number of the subcarriers and  $N=256$ ,  $w_0$  is the start of the stopband and can be set as  $2\pi/N$ ,  $TH$  is the threshold and be set as  $10^{-4}$ .

Following the optimization steps in paper [14], the designed prototype filter is shown in Fig. 4. From the comparison between PHYDYAS filter and optimized filter, they are almost same, only optimized filter has more impact on the neighboring symbol in time domain, which means that it has sharper spectrum in the frequency domain.

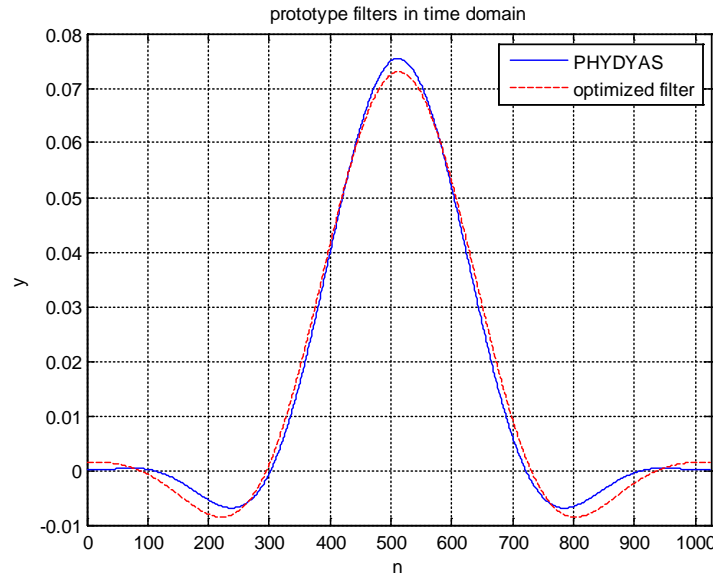


Fig. 4. The wave of optimized filter

Then, the spectrum of optimized filter is shown in Fig. 5. Compared to PHYDYAS filter in the Fig. 3, the main lobe bandwidth of the optimized filter (blue curve) is smaller than that of PHYDYAS filter (red dashed curve). Correspondingly, the side lobe of the optimized filter

is bigger than that of PHYDYAS filter. But, the energy of several side lobes neighboring to the main lobe is decreased rapidly. Rapidly decreased side lobes and narrow main lobe can keep the interference to neighboring subband at a very low level. This can be verified at the next simulation.

Also, in Fig. 5, there have other two curves, which are one subcarrier gap optimized filter (green curve) and half subcarrier gap optimized filter (black curve). The main lobes of optimized filter and one subcarrier gapped optimized filter are not even overlapped, which means there will be spectrum waste. However, the main lobes of optimized filter and half subcarrier gapped optimized filter are overlapped. The simulation in the next section will verify that the overlapped spectrum will not largely degrade the performance.

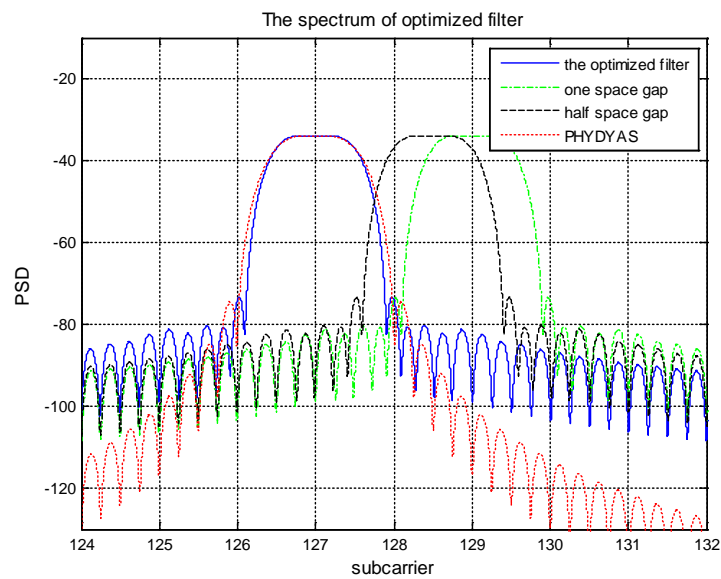


Fig. 5. The spectrum of optimized filter

Furthermore, in paper [18], a trans-multiplexer response is mentioned to show the interference to the neighboring time-frequency resource block. The trans-multiplexer response of PHYDYAS filter is shown in Table 1, in which,  $k, n$  represent the number of subcarrier and symbol in the time domain, respectively.

Table 1. PHYDYAS trans-multiplexer response with odd  $k'$

$\Delta k$	$\Delta n=-3$	$\Delta n=-2$	$\Delta n=-1$	$\Delta n=0$	$\Delta n=1$	$\Delta n=2$	$\Delta n=3$
$\Delta k=-1$	0.043j	-0.125j	-0.206j	$T_{-1,0}=0.239j$	0.206j	-0.125j	-0.043j
$\Delta k=0$	-0.067j	0	0.564j	$T_{0,0}=1$	0.564j	0	-0.067j
$\Delta k=1$	-0.043j	-0.125j	0.206j	$T_{1,0}=0.239j$	-0.206j	-0.125j	0.043j

The trans-multiplexer response is the output of FBMC when input data is set as '1', i.e.,  $d_{k,n}=1$ . When  $\Delta k \neq 0, \Delta n \neq 0$ , the elements of table represent the interference to the other time-frequency resource block. When  $\Delta k \neq 0$ , the interference represents the ICI interference in frequency domain. When  $\Delta n \neq 0$ , the interference represents ISI interference in time domain. From the Table 1, the interference is purely imaginary and can be cancelled by Re operation.



Corresponding, the trans-multiplexer response of the optimized prototype filter is shown in **Table 2**.

**Table 2.** The optimized filter's trans-multiplexer response with odd  $k'$

$\Delta k$	$\Delta n=-3$	$\Delta n=-2$	$\Delta n=-1$	$\Delta n=0$	$\Delta n=1$	$\Delta n=2$	$\Delta n=3$
$\Delta k=-1$	0.0711j	-0.1283j	-0.1768j	$T_{-1,0}=0.1942$	0.1768j	-0.1283	-0.0711j
$\Delta k=0$	-0.1009j	0.0003j	0.5874j	$T_{0,0}=0.9998$	0.5874j	0.0003j	-0.1009j
$\Delta k=1$	-0.0711j	-0.1283j	0.1768j	$T_{1,0}=0.1942$	-0.1768j	-0.1283	0.0711j

From comparison between **Table 1** and **Table 2**, the two tables are almost same, only some values are different. ICI interference (rows in the table) to the neighboring subcarrier is reduced in the **Table 2** of optimized filter trans-multiplexer response, while ISI interference (columns in the table) to neighboring symbols in time domain is enlarged. ICI reduction means the spectrum is shrinking, which is consistent with the analysis on **Fig. 5**. Spectrum shrinking will do good to enhance the spectral efficiency.

#### 4. Simulation results

To validate the good performance of the optimized filter and half subcarrier gap assignment scheme, we compare the different subcarrier gap schemes between the neighboring subbands with the optimized filter and the PHYDYAS filter. There are four different schemes: one subcarrier gap, half subcarrier gap, the quarter subcarrier gap, the zero-subcarrier gap between the neighboring subbands.

In the simulation, only BER performance is considered. Once BER performance satisfies the requirements, that means the half subcarrier gap scheme can work. If it can work, the spectral efficiency will be enlarged compared to traditional one subcarrier gap scheme in multi-user scenario.

The parameters of the simulation are as follows. The total number of subcarriers is 256 and the number of subcarriers in each subband is 4. The subband 1 starts from the 100th subcarrier. The signals transmitted on subband 1, 2, 3 are modulated with QPSK, 16QAM and 64QAM, respectively. Other subcarriers are kept as empty. The length of FBMC signals in every frame is 6. The channel is assumed as block flat Rayleigh distributed and independent. The detailed parameters are shown in **Table 3**.

**Table 3.** Simulation parameters

Parameters	value
Total subcarriers	256
The subcarriers in one subband	4
Modulation	QPSK/16QAM/64QAM
Subband 1	User 1, user 2
Subband 2	User 3, user 4
Subband 3	User 5, user 6
The number symbols of one frame	6 symbols
Channel of users	Independently block flat Rayleigh

The simulation is separated into two scenarios. One is that all users transmit at the same power. The other scenario is that the users in other subbands transmit at higher power leading to more interference to the focused user.

#### 4.1 Same power scenario

As shown in Fig. 6, The comparison results modulated with 4QAM of user 3 are presented.

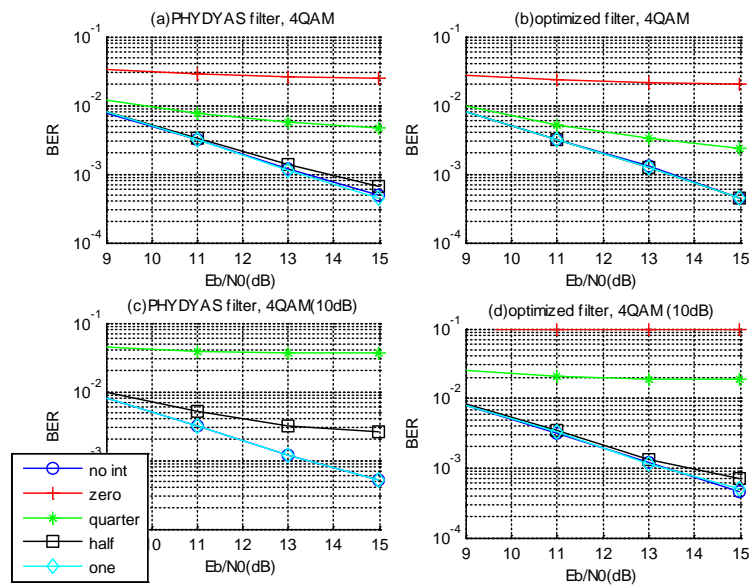


Fig. 6. The BER performance with 4QAM

In Fig. 6 (a), there are five BER performance curves with PHYDYAS filter, the curve without inter-subband interference (no int), the curve with one subcarrier gap (one), the curve with half subcarrier gap (half), the curve with the quarter subcarrier gap (quarter), the curve with zero subcarrier gap (zero). No interference means that data only transmits on subband 2 and subband 1 and 3 are empty.

It can be seen that the performance curve without inter-subband interference is the best since it has no overlap spectrum interference. Then the curve with one subcarrier gap performance curve is nearly almost the same with the curve without interference since the spectrum of PHYDYAS filter nearly occupies two subcarriers resulting to the neglected interference. The curve with half subcarrier gap is little worse than the curve with one subcarrier gap since the overlapped interference become larger. Finally, the curve with the quarter subcarrier gap is worse than the curve with half subcarrier gap and the curve with zero subcarrier gap is the worst, and both two curves show that these two schemes are not good to transmit the signals since the BER is at order of  $10^{-2}$ .

In **Fig. 6 (b)**, the performance curves with the optimized filter are similar to the curves with the PHYDYAS filter. The performance curve without the interference is the best and the curve with zero subcarrier gap is the worst. The curves with one subcarrier gap and the curve with half subcarrier gap are almost same as the curve without interference, which can show that the interference from the half subcarrier gapped subband can be neglected because the prototype filter has been optimized. Meanwhile, the curves with quarter subcarrier gap and zero subcarrier gap are better than that with PHYDYAS filter.

With the same power, the optimized filter and PHYDYAS filter both can work on half subcarrier scheme.

#### 4.2 Power control with more interference

Considering the power control will be used in downlink system, we consider the different transmission power on different subbands. In the simulation, we consider a worse scenario that the power of transmitted signal in the subband 1 and subband 3 is 10dB above the power of signal in the subband 2, which means subband 2 will encounter strong interference from subband 1 and 3. In this scenario, there will be much more interference on user 3.

The performance curves of this scenario are shown in **Fig. 6 (c)**. Compared to the **Fig. 6 (a)**, the curves without interference and with one subcarrier gap are the same as those in the **Fig. 6 (a)**. However, the curves with half subcarrier gap, quarter subcarrier gap and zero subcarrier gap are worse than those in the **Fig. 6 (a)** since the interference from neighboring subband is larger because of higher interference from the neighboring subband. Because of the much bad performance of the curve with zero subcarrier gap, the curve with zero subcarrier gap is not shown in **Fig. 6 (c)**.

Similar with **Fig. 6 (c)**, the curves of the optimized filter with power control are shown in **Fig. 6 (d)**. The trends of the curves of the optimized filter are similar with PHYDYAS filter. The main difference is that the curve with half subcarrier gap is approaching the curve with one subcarrier gap due to the optimized spectrum.

From the **Fig. 6**, in the strong interference scenario, the PHYDYAS filter with half subcarrier gap doesn't work well. However, combination of the half subcarrier gap assignment scheme with the optimized filter can still work well.

In high inter-interference scenario, the optimized filter can still work on half subcarrier scheme, but PHYDYAS filter cannot work on half subcarrier scheme.

#### 4.3 High order modulation

In this section, the simulation will be implemented in high order modulation. High order modulation needs high signal to interference noise ratio (SINR).

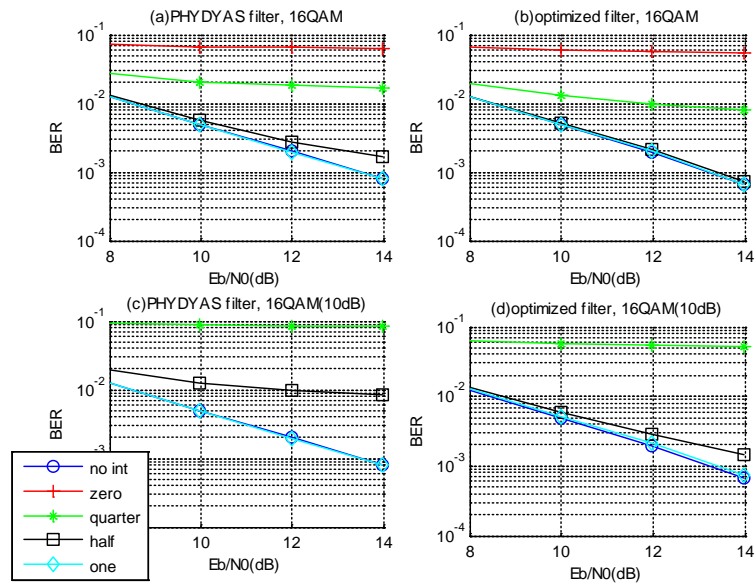


Fig. 7. The BER performance with 16QAM

The comparison of performance curves with 16QAM modulation is shown in Fig. 7. In Fig. 7 (a) and (b), PHYDYAS filter and optimized filter both work well in the half subcarrier gap scheme, the only difference is that PHYDYAS filter scheme has a little performance loss. It also can be seen that the PHYDYAS filter with half subcarrier gap scheme doesn't work well in the strong interference scenario in Fig. 7 (c). Instead, the half subcarrier gap scheme with the optimized filter can work well with little performance loss in the Fig. 7 (d).

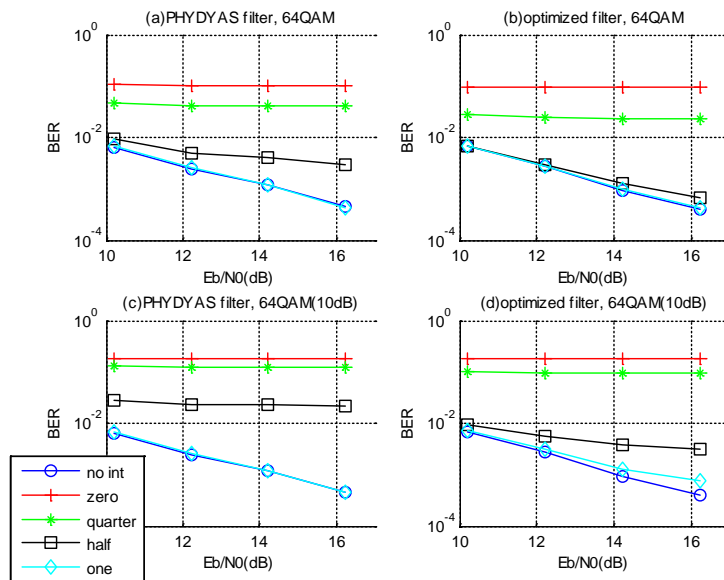


Fig. 8. The BER performance with 64QAM

The comparison of performance curves with 64QAM modulation is shown in **Fig. 8**. In **Fig. 8 (a)**, PHYDYAS filter with half subcarrier gap scheme has large performance loss. Instead, the optimized filter with the half subcarrier gap assignment scheme has a little performance loss in **Fig. 8 (b)**. In **Fig. 8 (c)**, PHYDYAS filter with half subcarrier does not work well. However, the half subcarrier gap assignment scheme can work with a few performance losses in **Fig. 8 (d)**. Though there have a few losses, but considering the high-order modulation and strong interference scenario, the performance still can be acceptable.

From the simulation results, the half subcarrier gap with high order modulation can work well with the optimized filter, even in the strong interference scenario.

## 5. Conclusion

In FBMC systems, the prototype filter is the key of the system performance. In this paper, consider the scenario of multi-user FBMC systems, in order to implement the resource assignment scheme of half subcarrier guard band, a new prototype filter is optimized. Compared to the traditional one subcarrier guard band scheme, half subcarrier scheme will improve the spectral efficiency, especially in the scenario of massive users.

According to the optimized method, we compare the optimized prototype filter and traditional PHYDYAS filter in time domain and frequency domain, as well as equivalent transmultiplexing response. The results show that the optimized filter has narrower spectrum. Furthermore, the link-level simulations about four different guard band assignment schemes have been done as well as with different modulation schemes and interference. The simulation results show that the combination of the half subcarrier guard gap spectrum assignment scheme with the optimized filter works well, even in the strong interference scenario.

## Acknowledgement

Thanks to the Prof. Qu Daiming for his thoughtful idea.

## References

- [1] R. Nissel, S. Schwarz and M. Rupp, "Filter Bank Multicarrier Modulation Schemes for Future Mobile Communications," *IEEE Journal on Selected Areas in Communications*, vol. 35, no. 8, pp. 1768-1782, Aug. 2017. [Article \(CrossRef Link\)](#)
- [2] W. Liu, D. Chen, K. Luo, T. Jiang and D. Qu, "FDM-Structured Preamble Optimization for Channel Estimation in MIMO-OQAM/FBMC Systems," *IEEE Transactions on Wireless Communications*, vol. 17, no. 12, pp. 8433-8443, Dec. 2018. [Article \(CrossRef Link\)](#)
- [3] J. Vihriala, N. Ermolova, E. Lahetkangas, et al., "On the Waveforms for 5G Mobile Broadband Communications," in *Proc. of 2015 IEEE 81st Vehicular Technology Conference (VTC Spring)*, pp. 1-5, 2015. [Article \(CrossRef Link\)](#)
- [4] B. Farhang-Boroujeny, "OFDM versus filter bank multicarrier," *IEEE Signal Processing Magazine*, vol. 28, no. 3, pp. 92-112, May 2011. [Article \(CrossRef Link\)](#)
- [5] P. Siohan, C. Siclet and N. Lacaille, "Analysis and Design of OFDM/OQAM Systems based on Filterbank Theory," *IEEE Transactions on Signal Processing*, vol. 50, no. 5, pp. 1170-1183, May 2002. [Article \(CrossRef Link\)](#)
- [6] B. Farhang-Boroujeny and C. H. Yuen, "Cosine Modulated and Offset QAM Filter Bank Multicarrier Techniques: A Continuous-Time Prospect," *EURASIP J. Adv. Signal Process*, 165654, 2010. [Article \(CrossRef Link\)](#)

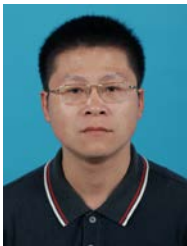
- [7] D. Mattera, M. Tanda and M. Bellanger, "Analysis of an FBMC/OQAM scheme for asynchronous access in wireless communications," *EURASIP Journal on Advances in Signal Processing*, vol. 2015, no. 23, March 2015. [Article \(CrossRef Link\)](#)
- [8] T. Ihalainen, A. Viholainen, T. H. Stitz, M. Renfors and M. Bellanger, "Filter bank based multi-mode multiple access scheme for wireless uplink," in *Proc. of 2009 17th European Signal Processing Conference*, pp. 1354-1358, 2009.
- [9] M. Bohge, F. Naghibi, A. Wolisz, "The use of guard bands to mitigate multiple access interference in the OFDMA uplink," in *Proc. of 13th international OFDM-Workshop*, pp. 75-79, Aug. 2008.
- [10] D. Gregoratti and X. Mestre, "Uplink FBMC/OQAM-Based Multiple Access Channel: Distortion Analysis Under Strong Frequency Selectivity," *IEEE Transactions on Signal Processing*, vol. 64, no. 16, pp. 4260-4272, 15 Aug. 15, 2016. [Article \(CrossRef Link\)](#)
- [11] M. Fuhrwerk, J. Peissig, M. Schellmann, "On the design of an FBMC based AIR interface enabling channel adaptive pulse shaping per sub-band," in *Proc. of 2015 23rd European Signal Processing Conference (EUSIPCO)*, pp. 384-388, 2015. [Article \(CrossRef Link\)](#)
- [12] D. Liu, Y. Liu, Z. Zhong, D. Miao, Z. Zhao and H. Guan, "5G uplink performance of filter bank multi-carrier," in *Proc. of 2016 IEEE 13th International Conference on Signal Processing (ICSP)*, pp. 1225-1230, 2016. [Article \(CrossRef Link\)](#)
- [13] Z. Zhao, X. Gong and M. Schellmann, "A Novel FBMC/OQAM Scheme Facilitating MIMO FDMA without the Need for Guard Bands," in *Proc. of WSA 2016; 20th International ITG Workshop on Smart Antennas*, pp. 1-5, 2016.
- [14] D. Chen, D. Qu, T. Jiang and Y. He, "Prototype Filter Optimization to Minimize Stopband Energy with NPR Constraint for Filter Bank Multicarrier Modulation Systems," *IEEE Transactions on Signal Processing*, vol. 61, no. 1, pp. 159-169, Jan.1, 2013. [Article \(CrossRef Link\)](#)
- [15] A. Şahin, İ. Güvenç and H. Arslan, "A comparative study of FBMC prototype filters in doubly dispersive channels," in *Proc. of 2012 IEEE Globecom Workshops*, pp. 197-203, 2012. [Article \(CrossRef Link\)](#)
- [16] M. Bellanger, "FBMC physical layer: a primer," [Online]. Available: [http://www.ict-phydyas.org/team-space/internal-folder/FBMC-Primer\\_06-2010.pdf](http://www.ict-phydyas.org/team-space/internal-folder/FBMC-Primer_06-2010.pdf), (Accessed: Nov. 2021).
- [17] R. Zakaria and D. Le Ruyet, "A novel FBMC scheme for Spatial Multiplexing with Maximum Likelihood detection," in *Proc. of 2010 7th International Symposium on Wireless Communication Systems*, pp. 461-465, 2010. [Article \(CrossRef Link\)](#)



**Wei Huang** received the B.S. degree in Communication Engineering from Wuhan University, Wuhan, China, in 2006, and the M.S. degree in Circuits and Systems from Wuhan University, in 2009. He is currently working toward the Ph.D. degree in Communication and Information System from Harbin Engineering University, Harbin, China. His research interests include wireless communications and signal processing.



**Hongbo Xu** received his Ph.D. degree in institute for pattern recognition artificial intelligence, Huazhong University of Science and Technology, Wuhan, China, in 2005. Since September 2005, he has been an associate professor in Central China Normal University. His main research interests include wireless communication and artificial intelligence.



**Zhongnian Li** received B.S. and M.S. telecommunication engineering degree from University of Electronics Science and Technology of China in 1998 and 2004. In 2009, he received Ph.D. degree in wireless communication major from Beijing University of Post and Telecommunication, China. Since 2009, he joined in Central China Normal University as a lecturer. His main research focuses on multi-carrier communication and massive MIMO.